CAMELOT - COMPUTATIONAL-ANALYTICAL MULTI-FIDELITY LOW-THRUST OPTIMISATION TOOLBOX

Marilena Di Carlo, Juan Manuel Romero Martin, Massimiliano Vasile

Department of Mechanical and Aerospace Engineering, University of Strathclyde, Glasgow, UK

ABSTRACT

CAMELOT (Computational-Analytical Multi-fidelity Low-thrust Optimisation Toolbox) is a toolbox for the fast preliminary design and optimisation of low-thrust trajectories. It solves highly complex combinatorial problems to plan multi-target missions characterised by long spirals including different perturbations. In order to do so, CAMELOT implements a novel multi-fidelity approach combining analytical surrogate modelling and accurate computational estimations of the mission cost. Decisions are then made by using two optimisation engines included in the toolbox, a single objective global optimiser and a combinatorial optimisation algorithm. CAMELOT has been applied to a variety of applications: from the design of interplanetary trajectories to the optimal deorbiting of space debris, from the deployment of constellations to on-orbit servicing. In this paper the main elements of CAMELOT are described and two space mission design problems solved using the toolbox are described.

Index Terms— Multi-target missions, low-thrust propulsion, combinatorial problems, multi-fidelity, surrogate models

1. INTRODUCTION

In recent years electric propulsion has become a key technology for space exploration and its use has increased in both near-Earth and interplanetary missions. Electric propulsion system have indeed the potential to provide shorter flight times, smaller launch vehicles and increased mass delivered to destination, when compared to high-thrust propulsion systems [1, 2].

Electric propulsion multi-target missions have been proposed in the literature [3, 4] and they are typical problems of the Global Trajectory Optimisation Competition (GTOC), [5].

The design of such missions require the definition of the best sequence of targets to visit and therefore the solution of a combinatorial optimisation problem. An additional difficulty in solving large combinatorial problems is the need to evaluate the cost of the transfer between targets several times. To quickly solve these problems it is therefore desirable to have a fast estimation for the cost of the transfer. When the model is expensive to evaluate, this estimation could be obtained through the use of surrogate models.

In this paper the Computational-Analytical Multi-fidelity Low-thrust Optimisation Toolbox (CAMELOT), a toolbox that combines the elements required to quickly design a low-thrust multi-target mission, is presented. CAMELOT includes multi-fidelity low-thrust transfer cost estimation, combinatorial optimisation solver, tools for the generation of surrogate models and single objective global optimiser. The combination of these elements allow to design a wide range of multi-target mission using electric propulsion: from the design of interplanetary trajectories to the optimal deorbiting of space debris, to the deployment of constellations.

In this paper two mission design applications of CAMELOT are presented: a multiple fly-by mission to the Atira astroids and an Active Debris Removal (ADR) mission to remove non-cooperative objects from Low Earth Orbit (LEO).

The paper starts with a description of the of the main tools of CAMELOT in Section 2. The two mission design applications are described in Section 3 and final remarks conclude the paper.

2. CAMELOT

The main components of CAMELOT are:

- Fast Analytical Boundary-value Low-thrust Estimator (FABLE);
- Multi Population Adaptive Differential Evolution Algorithm (MP-AIDEA);
- Automatic Incremental Decision Making And Planning algorithm (AIDMAP).

2.1. FABLE

FABLE provides accurate cost estimations (ΔV) of orbital transfers realized with electric propulsion using multi-fidelity analytical approach and surrogate models.

Low-fidelity tools give an estimation of the cost of the transfer using the analytic control laws summarized in Table 1; the variation of orbital elements corresponding to each law is described in the first column.

Table 1. Low-fidelity analytical control laws for the variation of orbital elements implemented in FABLE.

Transfer type	Reference
$a_0 \rightarrow a_f$	[6]
$(a_0, i_0) \rightarrow (a_f, i_f), e = 0$	[7]
$(a_0, i_0) \rightarrow (a_f, i_f), e = 0, a < \bar{a}$	[8]
$(a_0, \Omega_0) \rightarrow (a_f, \Omega_f), e = 0$	[8]
$(a_0, e_0, \omega_0) \rightarrow (a_f, e_f, \omega_f)$	[9]
$a_0 \rightarrow a_f, e_0 = e_f$	[10]
$e_0 \rightarrow e_f$	[6]
$e_0 \rightarrow e_f, a_f = a_0$	[10]
$(e_0, i_0) \rightarrow (e_f, i_f), a_f = a_0$	[11]
$i_0 \rightarrow i_f$	[6]
$\omega_0 \rightarrow \omega_f$	[6, 11, 12]
$\Omega_0 \rightarrow \Omega_f$	[6]

The higher-fidelity approach computes the ΔV using the analytical propagator implemented in FABLE. The analytical propagator is based on analytical formulas for the perturbed Keplerian motion obtained as results of a first-order expansion in the perturbing acceleration [13]. Using these formulas, osculating analytical propagator and averaged analytical propagator are implemented in FABLE. They include perturbations due to J2 zonal harmonic, atmospheric drag (modelled using the exponential atmospheric density model [14]), solar radiation pressure and low-thrust propulsion. Analytical solution are available for constant low-thrust acceleration and for constant tangential low-thrust acceleration [13]. The effect of shadow regions can also be included. Different control parameterisation can be implemented to compute low-thrust transfers.

When multi-target missions are considered the cost of the transfers between objects could have to be computed several times. In order to reduce the associated computational burden, FABLE can generate surrogate models of the transfers' cost to allow for a fast evaluation of complex trajectories. Surrogate models can be obtained using Kriging and the DACE toolbox [15] and Tchebycheff interpolation with sparse grid [16].

FABLE includes also tools for multi-fidelity optimisation of surrogate models. The optimisation is realized using the concept of co-Kriging and the maximisation of the expected improvement. The co-Kriging model allows to build an approximation of a function that is expensive to evaluate using data from low-fidelity model of the function [17]. The high-fidelity response $Z_{HF}(\mathbf{x})$ is approximated by multiplying the low-fidelity response $Z_{LF}(\mathbf{x})$ by a scaling factor, ρ, and a Gaussian process representing the difference between the high and low-fidelity data, $Z_D(\mathbf{x})$, [18]:

$$Z_{HF}(\mathbf{x}) = \rho Z_{LF}(\mathbf{x}) + Z_D(\mathbf{x}) \tag{1}$$

In FABLE the co-Kriging model is computed using ooDACE Toolbox [19].

The maximum expected improvement approach is used to locate the minimum of the function by finding the point where the likelihood of achieving an improvement, with respect to the current best function value, is maximized [20]. The expected improvement EI is defined as:

$$EI = s(\mathbf{x})\left[u\Phi(u) + \phi(u)\right] \tag{2}$$

where

$$u = \frac{f_{min} - \widehat{y(\mathbf{x})}}{s(\mathbf{x})} \tag{3}$$

In the previous equation $\widehat{y(\mathbf{x})}$ is the co-Kriging predictor, $s(\mathbf{x})$ is its error, Φ and ϕ are the normal cumulative distribution function and density function and f_{min} is the current best function value [20].

FABLE includes also astrodynamics tools for gravity assist, as shown in Section 3. Additional analytical capabilities include the possibility to compute the energy of the spacecraft subject to J2 and solar radiation pressure perturbations.

2.2. MP-AIDEA

Multi Population Adaptive Inflationary Differential Evolution Algorithm (MP-AIDEA) is a single objective global optimiser based on the combination of Differential Evolution (DE) [21] with local search and local and global restart procedures, [22]. The performance of the DE are strongly influenced by the setting of its two parameters, the differential weight F and the crossover probability CR, whose best settings are heavily problem dependent [23, 24]. In MP-AIDEA these parameters are automatically adapted during the optimisation. The DE is run until the populations contract below a given threshold. When the contraction condition is satisfied the DE is stopped and the algorithm decides whether to start or not a local search from the best individual of the population. This decision is taken based on the relative position of the best individual of the population with respect to the basin of attraction of previously detected local minima. The aim is to enable a transition from the current minimum to a neighboring one and to avoid multiple detections of the same local minima. If a local search is realized from the best individual of the population, the population is then locally restarted in a hypercube around the detected local minimum and the DE is started again. The dimension of the search space in which to locally restart the population is automatically adapted during the optimisation process. If no local search is realized the population is restarted globally in the whole search space at a distance from the clusters of local minima already detected. The local minima detected during the optimisation are saved in an archive of minima that allows to characterise the landscape of the function being minimized.

MP-AIDEA has been extensively tested over more than fifty test functions, including difficult academic test functions and real world test problems. Results have shown that the algorithm is averagely very efficient, being always in the first four positions in the ranking obtained comparing its results to those of others algorithms [22].

2.3. AIDMAP

The Automatic Incremental Decision Making And Planning algorithm (AIDMAP) is a single objective incremental decision making algorithm for the solution of complex combinatorial optimisation problems such as tasks planning and scheduling. AIDMAP works modeling the discrete decision making problems into a decision tree where nodes represent the possible decisions while links/edges represent the cost vector associated with the decisions. AIDMAP incrementally builds the decision tree from a database of elementary building blocks. These blocks represent a phase or leg of the mission. Using this approach eases the transcription of the problem into a tree-like topology. In addition, by incrementally building the decision tree, it is possible to prune the search space like proposed in [25, 26]. The decision tree is incrementally grown or explored by a set of Virtual Agents (VAs). The resulting decision tree is then evaluated by the VAs using a set of deterministic or probabilistic heuristics. The deterministic heuristics in AIDMAP are derived from classical Branch-and-Cut [27, 28] while the probabilistic heuristics are bio-inspired and mimic the evolution of the slime mold Physarum Polycephalum, a simple single cell organism endowed by nature with a simple but powerful heuristic that can solve complex discrete decision making problems [29, 30, 31]. Unlike Branch-and-Cut, that uses a set of deterministic branching and pruning heuristics, the Physarum algorithm uses probabilistic heuristics to decide to branch or prune a vein. Branches are never really pruned but the probability of selecting them may fall to almost zero. The mechanism of Physarum is analogous to the most commonly known Ant Colony Optimisation algorithm [30]. A more detailed description of the Physarum is given in [32].

AIDMAP has been extensively tested on a variety of Travelling Salesman and Vehicle Routing problems, providing good results [14, 32, 33].

3. APPLICATIONS

CAMELOT can be applied to different mission design problems. Here, a multiple asteroid fly-by mission and a multiple active debris removal mission are presented.

3.1. Multiple asteroids fly-by mission

The first application of CAMELOT is the design of a mission to visit the Atira asteroids [34]. Atira asteroids are Near-Earth Asteroids (NEAs) with both perihelion and aphelion within the orbit of the Earth (semimajor axis $a < 1$ AU and aphelion $Q < 0.983$ AU), also called Inner-Earth Objects (IEOs).

The first Atira object was discovered in 2003 and, as of December 2014, only fourteen asteroids are counted in this group. However, many more objects are expected to exist in the same region of the Solar System. To date, over eleven thousand NEAs have been identified, the majority of which are characterized by semimajor axis greater than 1 AU, as shown in Figure 1, where the distribution of the known NEAs is shown in the a-e plane, with the Atira asteroids represented in red. Inner Solar System asteroids are difficult to detect because of the limitations of ground-based survey: telescopes can only search on the night side of the Earth, where the Sun is not in the field of view.

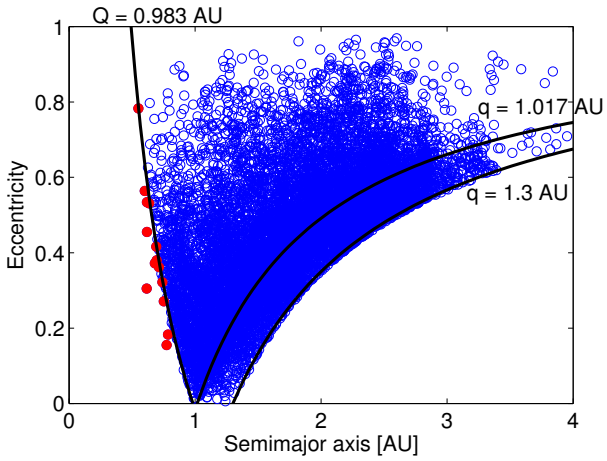

Fig. 1. NEAs distribution - red circles indicate Atira asteroids.

The proposed mission visits the Atira asteroids by making use of an electric propulsion system. To maximize the scientific return of the spacecraft, the mission is optimized to visit the maximum possible number of asteroids of the Atira group. The encounters with the asteroids are realized through a series of fly-bys at the nodal points of their orbits. This strategy allows avoiding out-of-plane maneuvers for the change of inclination; the 14 Atira asteroids have inclination ranging from 0 to 30 degrees.

The design of the mission is divided into three phases:

1. Identification of the optimal asteroid sequence and the optimal departure and arrival dates, using AIDMAP and an impulsive Lambert model for the transfer;

2. Refinement of the optimal solution identified by AIDMAP using MP-AIDEA;

3. Translation of the identified optimal solution into a low-thrust optimal trajectory using FABLE.

In the first step AIDMAP is used to identify the optimal sequence of asteroids to visit and the optimal departure and arrival dates, considering a 10 years mission time span from 01 January 2020 to 01 January 2030. The trajectories between asteroids are composed of sequences of conic arcs linked together through discrete, instantaneous events. Each conic arc is the solution of a Lambert problem, which is solved to compute the ΔV required for the transfer to reach each asteroid at its nodal point. The arrival conditions are defined by the passage of the asteroids through their nodal points and the departure conditions are identified, on the departure orbit, by a minimum and maximum value for the time of flight to reach the nodal point, [34]. AIDMAP identifies 133,761 possible solutions. A filtering process is applied to identify solutions with different sequence of targeted asteroids. After the filtering, fourteen unique solutions visiting six asteroids and fifty-seven unique solutions visiting five asteroids are found. The best solution found by AIDMAP, that is the one characterized by the maximum number of asteroid visited and the lowest total ΔV, has six fly-bys based on the following sequence of asteroids visited: Earth - 2013JX28 - 2006WE4 - 2004JG6 - 2012VE46 - 2004XZ130 - 2008UL90 . The total ΔV cost, obtained from a Lambert model, is 3.77 km/s and the transfer time is 8.4 years. More details about this solutions are reported in Table 2.

The best solution identified by AIDMAP is then further optimized using the global optimiser MP-AIDEA. For the additional optimisation, a local window of 10 days is allocated around the previous defined departure dates in order to identify new departures dates leading to an improved result in term of total ΔV. The obtained results are reported in Table 3, showing a reduction of 0.16 km/s in the total ΔV with respect to the results presented in Table 2.

In the last phase of the mission design FABLE is used to optimise the low-thrust transfer between the previously defined asteroids nodes. A direct optimisation method and multiple shooting algorithm are used. In the multiple shooting algorithm, the trajectory is segmented into legs that begin and end at On/Off control nodes, where On nodes define the switching point from null thrust to maximum thrust and Off nodes define the switching point from maximum thrust to null thrust The state vectors corresponding to each node are determined by the optimisation process, being treated as optimisables controls [35]. The trajectory is therefore segmented into a sequence of thrust and coast legs. A middle point is defined for each transfer and the state vector is forward-propagated on each of the legs from the departure point to the mid point and back-propagated on each of the legs from the arrival point (that is, the asteroid nodal point) to the mid point. Keplerian motion is considered on the coast legs, while on the thrust legs the analytical model for the propagation of the orbital motion under low-thrust perturbation included in FABLE is used. The initial acceleration is set at $10^{-4}\mathrm{m/s}^2$, equivalent to a thrust of T = 0.07 N applied to a 700 kg spacecraft. The specific impulse considered is Isp = 3000 s. The spacecraft is injected into an interplanetary orbit which allows it to realize the first fly-by without switching on the engine. After the first fly-by the engine can be switched on to achieve the remaining five fly-bys. The results of the optimised low-thrust transfers are reported in Table 4 and shown in Figure 2, where the thrust legs are in black and the coast legs are in grey.

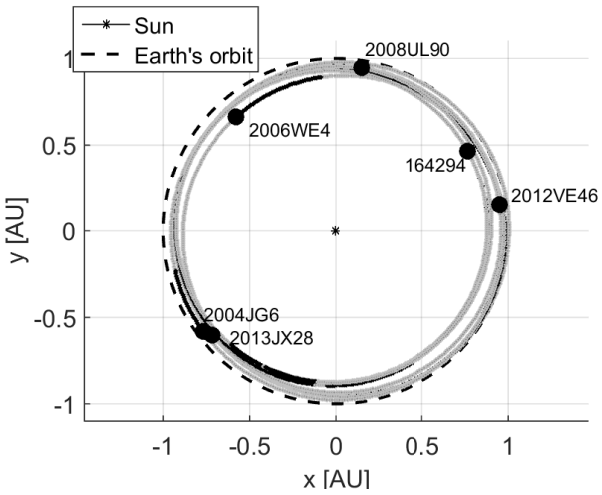

Fig. 2. Trajectory for multiple fly-by of the Atira asteroids.

After the last fly-by the spacecraft is moved on an parking orbit with lower perihelion (0.725 AU). This allows the spacecraft to move to inner regions of the solar Systems to search for new NEAs. Two strategies to realise this transfer are considered. In the first one the low-thrust engine is used to alternate coast and thrust arc so as to reach the final parking orbit with the minimum ΔV (Figure 3); in the second case the spacecraft is moved on an orbit that intersect the Earth's one, so that a gravity assist with the Earth can be obtained (Figure 4). The transfer in Figure 3 is realized in 422 days and requires $\Delta V = 1.8$ km/s. The transfer realized through gravity-assist with the Earth takes 565 days but requires $\Delta V = 1.31$ km/s.

3.2. Multiple Active Debris Removal Mission

The second proposed application of CAMELOT is the design of a mission to de-orbit non-cooperative large satellites from Low Earth Orbit (LEO). The recent growth of space debris population represents a collision threat for satellite and manned spacecraft in Earth orbit. Recent studies have concluded that regions within LEO have already reached a critical density of objects which will eventually lead to a cascading process known as the Kessler syndrome [36]. The Inter-Agency Space Debris Coordination Committee has issued guidelines to mitigate the growth of space debris [37]. However it has been proved that compliance with these recommendations will not stop the exponential growth and that

Table 2. Best solution obtained with six visited asteroids using AIDMAP with Lambert model.

	Asteroid	Departure Date Lambert Arc	ToF Lambert Arc [days]	Arrival Date at Asteroid Node	ΔV [km/s]
	2013JX28	2020/09/29	205	2021/04/22	0.87
	2006WE4	2022/05/14	215	2022/12/15	0.86
	2004JG6	2023/06/14	235	2024/02/04	0.61
	2012VE46	2024/09/11	265	2025/06/03	0.36
	2004XZ130	2026/09/15	205	2027/04/08	0.73
	2008UL90	2028/07/31	195	2029/02/11	0.34
TOTAL					3.77

Table 3. Further optimisation of the best solution obtained with six visited asteroids using MP-AIDEA.

	Asteroid	Departure Date Lambert Arc	ToF Lambert Arc [days]	Arrival Date at Asteroid Node	ΔV [km/s]
	2013JX28	2020/09/20	214.5329	2021/04/22	0.95
	2006WE4	2022/05/24	205	2022/12/15	0.69
	2004JG6	2023/06/12	236.2514	2024/02/04	0.61
	2012VE46	2024/09/05	270.6114	2025/06/03	0.34
	2004XZ130	2026/09/18	201.5318	2027/04/08	0.72
	2008UL90	2028/08/10	185.0003	2029/02/11	0.29
TOTAL					3.61

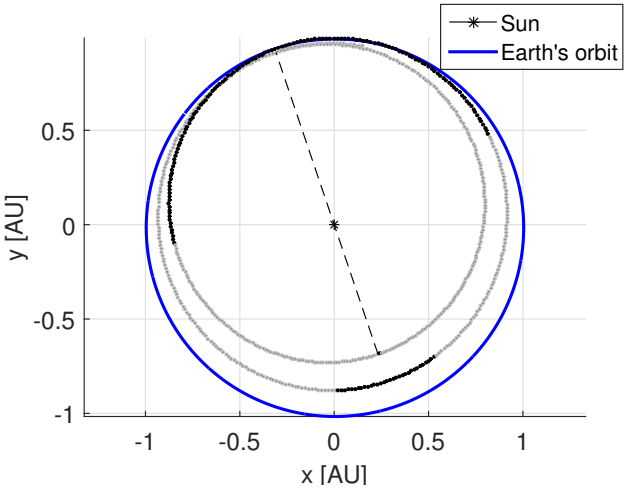

Fig. 3. Trajectory for transfer to reduced perigee parking orbit.

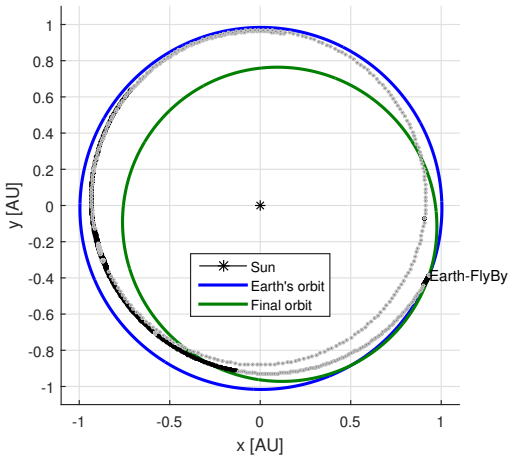

Fig. 4. Trajectory for transfer to reduced perigee parking orbit using a gravity assist with the Earth.

the active removal of five to ten large objects per year is required to stabilize the population [38].

In this study a single servicing spacecraft equipped with electric engine is used for the de-orbiting of large satellites from the region between 800 and 1400 km in LEO. Two removal approaches are considered:

- Multi-target delivery of de-orbiting kits to perform a controlled re-entry;
- Low-thrust fetch and de-orbit using the single towing spacecraft.

The possible targets to be removed are selected from the catalogue of the current objects in LEO regularly maintained by the North American Aerospace Defence Command (NORAD). Using the NORAD catalogue, 721 objects in the range 800-1400 km and characterized by Radar Cross Section greater than 1 are found, [14]. The potential 721 target

Table 4. Summary of leg-by-leg simulation results for optimal, six-leg, low-thrust trajectory.

	Asteroid	Time Engine On [days]	m_0 [kg]	m_f [kg]	ΔV [km/s]
	2013JX28	0	700	700	-
	2006WE4	129.05	700	673.45	1.12
	2004JG6	152.57	673.45	642.07	1.37
	2012VE46	41.77	642.07	633.47	0.40
	2004XZ130	158.40	633.47	600.89	1.51
	2008UL90	30.04	600.89	594.17	0.30
TOTAL					4.70

objects are then further selected based on two main criteria: the rate of the drift of the right ascension of the ascending node due to the second zonal harmonic of the gravity, J2, and the Criticality of Spacecraft Index (CSI), [39].

The change of right ascension, when realizing a transfer between two satellites, is realized by changing the semimajor axis of the servicing spacecraft and taking advantage of the dependence on the altitude of the natural rate of nodal regression due to J2 [11]. Smaller inclination orbits are more favorable for adjustment of right ascension realized by changing the semimajor axis [14], therefore the group of object with lower possible inclination is selected.

The targets are also selected based on their value of the Criticality of Spacecraft Index, which expresses the environmental criticality of objects in LEO taking into account the physical characteristics of a given object, its orbit and the environment where it is located. After applying these selection criteria, a set of 25 objects are selected. The selected 25 objects for this study are among the 100 most critical objects in term of CSI [39]; the apogee and perigee altitude and inclination of the selected targets (highlighted in the circle) are shown in Figure 5.

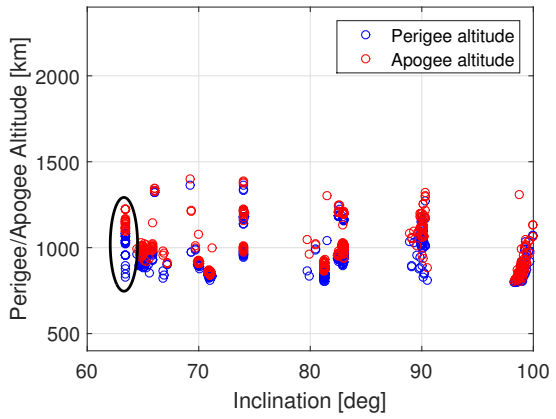

Fig. 5. Selected objects in LEO.

Once the database of objects is defined, the identification of the optimal sequence of targets to be removed is realized using AIDMAP and a surrogate model of the cost (ΔV) of the transfer of the low-thrust servicing spacecraft between objects, obtained using FABLE.

For the computation of the cost associated to transfers between two satellites, the total transfer is divided into two phases [14]:

- in the first phase an optimisation problem is solved in order to adjust e, i and ω in a given time of flight with the minimum propellant consumption;
- in the second phase a and Ω are adjusted, while keeping i and e equal to the target's ones and constraining ω to match the final argument of the perigee of the target orbit.

More details about the transfer model can be found in [14]. For the multi-target delivery of de-orbiting kits strategy, the sequence of transfer characterized by the lower total time of flight is reported in Table 5. Ten satellites, identified in Table 5 by their NORAD ID, can be serviced in less than one year. m_0 is the initial mass for the transfer and m_f the mass at the end of the transfer. The 100 kg drop in mass after each transfer accounts for the attachment of the de-orbiting kit to the serviced satellite. ToF represents the time of flight required to realize the transfer and T_w represents the waiting time on the orbit of the departure object required to obtain the orbital phasing with the arrival satellite. Figures 6 and 7 show the variation of orbital elements during the transfer from object 40342 to object 40338. These figures show how the use of the natural dynamics (J2) can be exploited to reach the desired value of Ω.

When the servicing spacecraft is used to fetch and de-orbit a non-cooperative satellite, the results presented in Table 6, for a mission with ToF of 373 days, are found. In this case three satellites can be removed from LEO. Figure 8 shows the variation of perigee altitude of the servicing spacecraft (grabbing object 36413 during the deorbiting phase) and the subsequent orbit raising phase. The total time required is 180.02 days. The shorter orbit raising time is due to the fact that, when the perigee reaches 300 km, the servicing spacecraft

Table 5. Sequence of removed satellite for servicing spacecraft delivering de-orbiting kits.

	Departure Object	Arrival Object	ΔV [km/s]	ToF [days]	$T_{w,\theta}$ [hours]	m_0 [kg]	m_f [kg]
1	39015	40343	0.0628	30.43	2.59	1900.00	1892.40
2	40343	40340	0.1128	65.75	1.78	1792.40	1779.55
3	40340	39016	0.0595	33.14	2.54	1679.55	1673.19
4	39016	40342	0.0429	29.73	2.70	1573.19	1568.89
5	40342	40338	0.0339	42.28	2.06	1468.89	1465.72
6	40338	40339	0.0013	7.05	1.78	1365.72	1365.60
7	40339	39011	0.1116	44.55	2.43	1265.60	1256.63
8	39011	39012	0.0035	14.19	2.07	1156.63	1156.37
9	39012	39013	0.0448	28.04	2.07	1056.37	1053.34
Total	-	-	0.4731	294.17	20.04	-	-

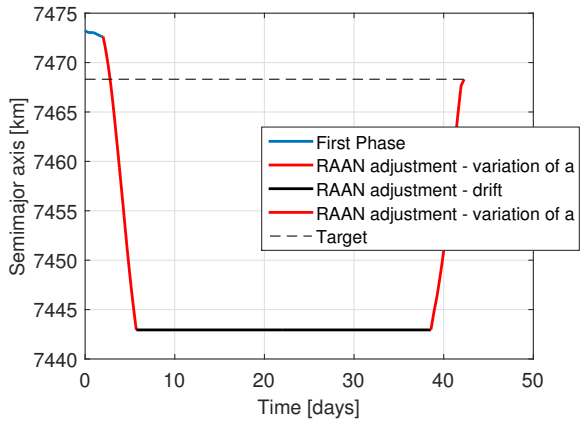

Fig. 6. Variation of a during transfer from object 40342 to object 40338.

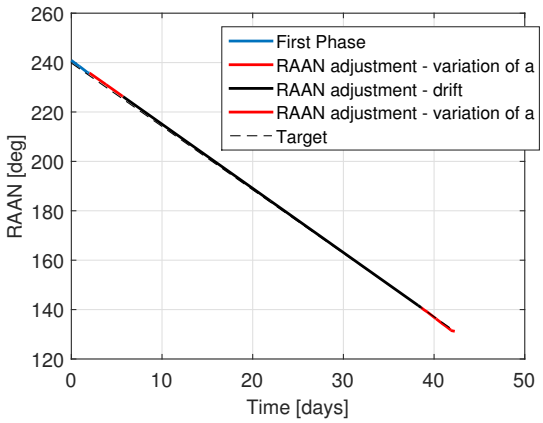

Fig. 7. Variation of Ω during transfer from object 40342 to object 40338.

dispose of the 2000 kg serviced satellites and this results in an increased acceleration in the raising phase. The deorbiting is realized using continuous negative tangential acceleration while the orbit raising is performed with continuous positive tangential acceleration. The tools implemented in FABLE allow to realise the deorbiting also by increasing the eccentricity of the orbit, applying a negative tangential thrust at apogee and a positive tangential thrust at perigee. In this case the re-entry conditions will be different from the ones obtained deorbiting with continuous tangential acceleration because of the increased eccentricity of the re-entry orbit (the fligth path angle at re-entry increases from ≈ 0 to 1.5 deg). The variation of perigee and apogee altitude in this case is shown in Figure 9.

An application of the multi-fidelity optimisation of surrogate models described in Section 2.1 can be considered by looking at the first transfer between satellite deorbited by means of de-orbiting kits. As reported in Table 5 the transfer is from object 39015 to object 40343. A surrogate model of the ΔV required to realize this transfer, using different times of flight and different initial masses of the spacecraft, is shown in Figure 10. This surrogate model is generated using Kriging and the Matlab DACE tool by sampling uniformly the parameter space. The surrogate model obtained is then used by AIDMAP for the definition of the optimal sequence of satellite to deorbit. A rigorous and time-consuming sampling of the expensive high-fidelity model is not necessary, however, if the aim is only to locate the minimum cost of the transfer. In this case an analytical model for the cost of the transfer between two satellites can be used as a low-fidelity representation of the problem. The low-fidelity model makes use of the analytical laws in Table 1. A co-Kriging model of the function is then build by using data from the low-fidelity model and few data points from the higher-fidelity model. The co-Kriging representation of the cost of the transfer, obtained using 20 low-fidelity points and 3 expensive higher-fidelity points is shown in Figure 11. The point where the expected improvement is maximized is then located using

Table 6. Sequence of removed satellite for servicing satellite fetching non-operational satellite.

	Departure Object	Arrival Object	ΔV [km/s]	ToF [days]	$T_{w,\theta}$ [hours]	m_0 [kg]	m_f [kg]
1	39244	36413	1.1307	159.91	2.09	3000.00	890.11
2	36413	39011	0.9811	182.32	2.41	2890.11	802.79
Total	-	-	2.6118	373.23	4.5	-	-

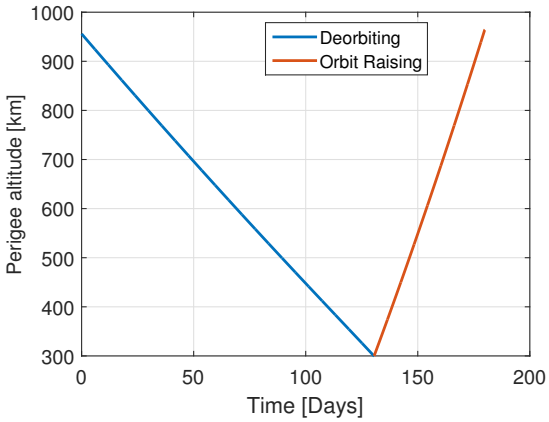

Fig. 8. Variation of the perigee altitude for the servicing spacecraft during deorbit of object 36413 and orbit raising to the semimajor axis of target object 39011.

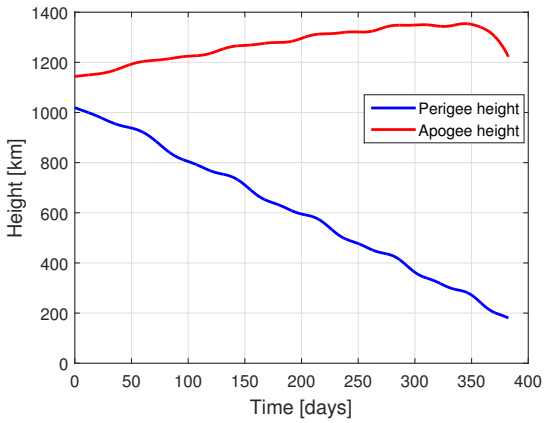

Fig. 9. Variation of perigee and apogee altitude for re-entry with increase of eccentricity.

MP-AIDEA. The high-fidelity function is evaluated in the point of maximum expected improvement, the co-Kriging surrogate model is computed again and the process is repeated. The representation of the expected improvement at the first step of the iterative procedure is shown in Figure 12.

The iteration stops after three runs, corresponding to three additional sampling in the most promising area (high time of flight, low spacecraft mass), when the expected improvement is lower than a pre-defined value. The Co-Kriging surrogate model at the end of the iterative process is shown in Figure 13. The minimum is correctly located at $m = 600$ kg and time of flight equal to 122 days.

4. CONCLUSION

In this paper CAMELOT, a toolbox for the design and optimisation of multi-target low-thrust trajectories mission, has been presented. The three main components of CAMELOT, FABLE, MP-AIDEA and AIDMAP have been described. The toolbox has been applied to two case studies, the design of an interplanetary trajectory to visit the Atira asteroids and the design of a mission to deorbit multiple non-cooperative objects from LEO. Results have shown that CAMELOT can solve different space problems in an efficient way while remaining easily adaptable to different applications.

5. ACKNOWLEDGMENTS

This research was partially supported by Airbus Defence and Space. The authors would like to thank Mr. Stephen Kemble for his support and contribution.

6. REFERENCES

[1] S. N. Williams and V. Coverstone-Carroll, "Benefits of solar electric propulsion for the next generation of planetary exploration missions," *Journal of the Astronautical Sciences*, vol. 45, no. 2, pp. 143–159, 1997.

[2] C. G. Sauer and C. W. L Yen, "Planetary mission capability of small low power solar electric propulsion systems," *Acta Astronautica*, vol. 35, pp. 625–634, 1995.

[3] J.T. Olympio and N. Frouvelle, "Space debris selection and optimal guidance for removal in the SSO with low-thrust propulsion," *Acta Astronautica*, vol. 99, pp. 263–275, jun 2014.

[4] M. Cerf, "Multiple space debris collecting mission. debris selection and trajectory optimization," .

[5] "The global trajectory optimisation competition portal," http://sophia.estec.esa.int/gtoc_portal/, Accessed: 2016-02-22.

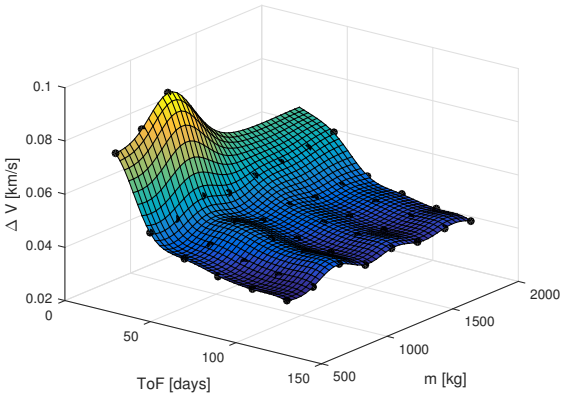

Fig. 10. Surrogate model of the cost of the transfer between objects 39015 and 40343.

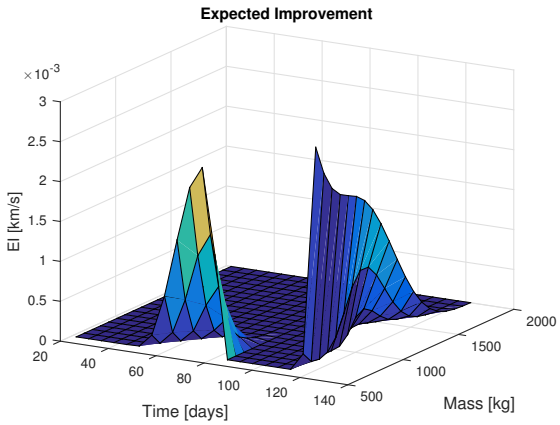

Fig. 12. Expected improvement for the surrogate model of the cost of the transfer between objects 39015 and 40343.

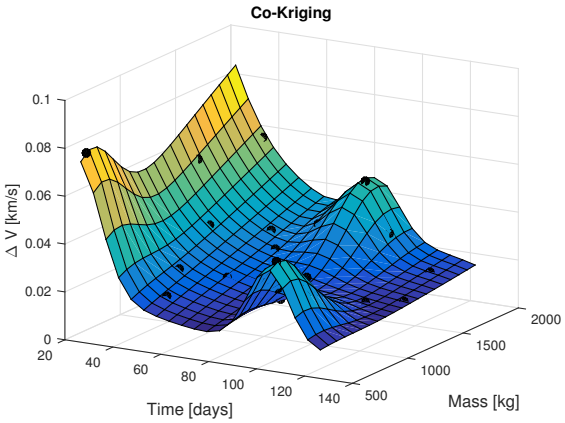

Fig. 11. Co-Kriging surrogate model of the cost of the transfer between objects 39015 and 40343.

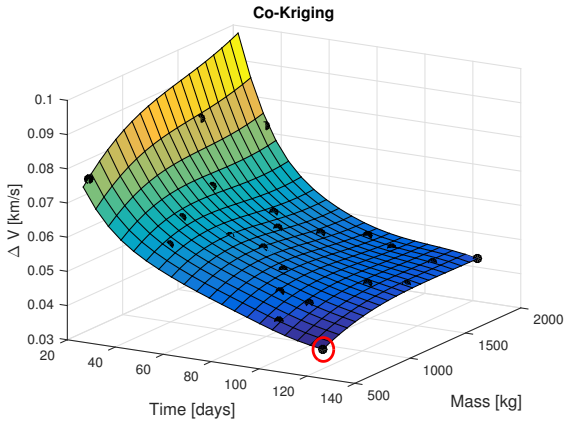

Fig. 13. Co-Kriging surrogate model at the last iteration of the maximization of the expected improvement.

[6] A. Ruggiero, P. Pergola, S. Marcuccio, and M. Andrenucci, "Low-thrust maneuvers for the efficient correction of orbital elements," in *32nd International Electric Propulsion Conference*, 2011, pp. 1–13.

[7] T. N. Edelbaum, "Propulsion requirements for controllable satellites," *ARS Journal*, vol. 31, no. 8, pp. 1079–1089, 1961.

[8] J. A. Kéchichian, "Analytic representations of optimal low thrust transfer in circular orbits," *Spacecraft Trajectory Optimization*, vol. 29, pp. 139, 2010.

[9] S. da Silva Fernandes, F. das Chagas Carvalho, and R. V. de Moraes, "Optimal low-thrust transfers between coplanar orbits with small eccentricities," *Computational and Applied Mathematics*, pp. 1–14, 2015.

[10] E. G. C. Burt, "On space manoeuvres with continuous thrust," *Planetary and Space Science*, vol. 15, no. 1, pp. 103–122, 1967.

[11] J. E. Pollard, "Simplified analysis of low-thrust orbital maneuvers," Tech. Rep., DTIC Document, 2000.

[12] A. E. Petropoulos, "Simple control laws for low-thrust orbit transfers," 2003.

[13] F. Zuiani and M. Vasile, "Extended analytical formulas for the perturbed keplerian motion under a constant control acceleration," *Celestial Mechanics and Dynamical Astronomy*, vol. 121, no. 3, pp. 275–300, 2015.

[14] J. M. Romero Martin, M. Di Carlo, and M. Vasile, "Automatic planning and scheduling of active removal of non-operational satellites in low earth orbit," in *66st International Astronautical Congress, IAC 2015*, 2015, pp. Paper–IAC.

[15] S. N. Lophaven, H. B. Nielsen, and J. Søndergaard, "Dace-a matlab kriging toolbox, version 2.0," Tech. Rep., 2002.

[16] C. Ortega, A. Riccardi, M. Vasile, and C. Tardioli, "Smart-uq: Uncertainty quantification toolbox for generalized intrusive and non intrusive polynomial algebra," in *6th ICATT*, 2016.

[17] A. I. J. Forrester, A. Sóbester, and A. J. Keane, "Multi-fidelity optimization via surrogate modelling," in *Proceedings of the royal society of london a: mathematical, physical and engineering sciences*. The Royal Society, 2007, vol. 463, pp. 3251–3269.

[18] D. J. J. Toal, "Some considerations regarding the use of multi-fidelity kriging in the construction of surrogate models," *Structural and Multidisciplinary Optimization*, vol. 51, no. 6, pp. 1223–1245, 2015.

[19] I. Couckuyt, T. Dhaene, and P. Demeester, "oodace toolbox: a flexible object-oriented kriging implementation," *The Journal of Machine Learning Research*, vol. 15, no. 1, pp. 3183–3186, 2014.

[20] D. R. Jones, "A taxonomy of global optimization methods based on response surfaces," *Journal of global optimization*, vol. 21, no. 4, pp. 345–383, 2001.

[21] K. Price, R. M. Storn, and J. A. Lampinen, *Differential evolution: a practical approach to global optimization*, Springer Science & Business Media, 2006.

[22] M. Di Carlo, M. Vasile, and E. Minisci, "Multi-population inflationary differential evolution algorithm with adaptive local restart," in *2015 IEEE Congress on Evolutionary Computation (CEC)*. IEEE, 2015, pp. 632–639.

[23] S. Das and P. N. Suganthan, "Differential evolution: a survey of the state-of-the-art," *IEEE Transactions on Evolutionary Computation*, vol. 15, no. 1, pp. 4–31, 2011.

[24] R. Gämperle, S. D. Müller, and P. Koumoutsakos, "A parameter study for differential evolution," *Advances in intelligent systems, fuzzy systems, evolutionary computation*, vol. 10, pp. 293–298, 2002.

[25] V. M. Becerra, D. R. Myatt, S. J. Nasuto, J. M. Bishop, and D. Izzo, "An efficient pruning technique for the global optimisation of multiple gravity assist trajectories," *Acta Futura*, vol. 2005, pp. 35, 2003.

[26] D. Novak and M. Vasile, "Incremental solution of lt-mga transfers transcribed with and advanced shaping approach," in *International Astronautical Congress*, Prague, 27 September - 01 October 2010.

[27] M. Jepsen, B. Petersen, and S. Spoorendonk, "A branch-and-cut algorithm for the elementary shortest path problem with a capacity constraint," *Department of Computer Science, . . . ,* , no. 08, 2008.

[28] S. Volker, "Formulations and branch-and-cut algorithms for the generalized vehicle routing problem," *Investment Management and Financial Innovations*, vol. 5, no. 4, pp. 7–24, 2014.

[29] T. Nakagaki, H. Yamada, and Á. Tóth, "Intelligence: Maze-solving by an amoeboid organism," *Nature*, vol. 407, no. 6803, pp. 470–470, 2000.

[30] D. S. Hickey and L. A. Noriega, "Insights into information processing by the single cell slime mold physarum polycephalum," in *UKACC Control Conference*, 2008, pp. 2–4.

[31] R. Kobayashi T. Saigusa T. Nakagaki A. Tero, K. Yumiki, "Flow-network adaptation in physarum amoebae," *Theory in Biosciences*, vol. 127, no. 2, pp. 98–94, 2008.

[32] J. M. Romero Martin, L. Masi, M. Vasile, E. Minisci, R. Epenoy, V. Martinot, and J. Fontdecaba Baig, "Incremental planning of multi-gravity assist trajectories," in *65st International Astronautical Congress, IAC 2014*, 2014, pp. Paper–IAC.

[33] L. Masi and M. Vasile, "A multidirectional physarum solver for the automated design of space trajectories," July 6-11, 2014.

[34] M. Di Carlo, N. Ortiz Gómez, J. M. Romero Martin, C. Tardioli, F. Gachet, K. Kumar, and M. Vasile, "Optimized low-thrust mission to the atira asteroids," in *25th AAS/AIAA Space Flight Mechanics Meeting*, 2015, pp. AAS15–299.

[35] S. Kemble, *Interplanetary mission analysis and design*, Springer Science & Business Media, 2006.

[36] D. J. Kessler, N. L. Johnson, J.C. Liou, and M. Matney, "The kessler syndrome: implications to future space operations," *Advances in the Astronautical Sciences*, vol. 137, no. 8, pp. 2010, 2010.

[37] Inter-Agency Space Debris Coordination Committee et al., *IADC space debris mitigation guidelines*, Inter-Agency Space Debris Coordination Committee, 2002.

[38] J-C Liou and Nicholas L Johnson, "Instability of the present leo satellite populations," *Advances in Space Research*, vol. 41, no. 7, pp. 1046–1053, 2008.

[39] A. Rossi, G. B. Valsecchi, and E. M. Alessi, "The criticality of spacecraft index," *Advances in Space Research*, vol. 56, no. 3, pp. 449–460, 2015.